岩手医科大学
審査学位論文
(博　士)

Longitudinal systolic strain of the bilayered ventricular septum

during the first 72 h of life in preterm infants

Yurie Nasu・Kotaro Oyama・Satoshi Nakano・Atsushi Matsumoto・Wataru Soda・

Shin Takahashi・Shoichi Chida

Department of Pediatrics, Iwate Medical University School of Medicine

Corresponding author:

Y Nasu, Department of Pediatrics, Iwate Medical University School of Medicine

19-1 Uchimaru, Morioka, Iwate 020-8505, Japan

Tel: +81-19-651-5111; Fax: +81-19-624-8384

Email: yurienas@iwate-med.ac.jp

Abstract

Background Quantitative evaluation of right ventricular myocardial performance in preterm infants remains a challenge because of the limitations of conventional echocardiographic measurement and the complex geometry of the right ventricle (RV). Serial assessment of peak longitudinal systolic strain on the right and left sides of the ventricular septum (VS), RV, and left ventricle (LV) during the transitional period in preterm infants using two-dimensional speckle-tracking echocardiography is reported.

Methods In 21 preterm infants (33 ± 2 gestational weeks, 1913 ± 218 g birth weight without mechanical ventilation, inotropic agents, or symptomatic patent ductus arteriosus (PDA), longitudinal strain (LS) was measured on both sides of the VS, RV free wall, and LV, along with conventional echocardiography at 1, 3, 6, 9, 12, 24, 48, and 72 h after birth. Correlations and factors associated with echocardiographic measurements were analyzed.

Results LS was maintained on the four analyzed regions during the first 72 h of life despite significant hemodynamic changes, including a decrease in pulmonary artery pressure and PDA closure. LS was significantly larger on the left side of the VS than on the right side of the VS at 1, 48, and 72 h after birth.

Conclusions Preterm infants showed stable LS on both sides of the VS, the RV free wall, and the LV despite significant hemodynamic changes during the first 72 h of life. These results suggest that the right and left sides of the VS respond differently to the complex cardiopulmonary transitions from fetal to neonatal life in preterm infants.

Key words: two-dimensional speckle-tracking echocardiography, strain, ventricular septum, preterm infants

Introduction

The transition from fetal to neonatal life is characterized by major circulatory alterations: a decrease in pulmonary vascular resistance, an increase in pulmonary blood flow, and closure of fetal shunts. Preterm infants are susceptible to hemodynamic derangements, such as hypotension and hemodynamically significant patent ductus arteriosus (PDA) during this period [1, 2]. Serial assessment of both right and left ventricular myocardial adaptation during the transition would be helpful for optimal cardiovascular management of preterm infants [1-4]. However, quantitative evaluation of right ventricular myocardial performance in preterm infants remains a challenge because of the limitations of conventional echocardiographic measurement and the complex geometry of the right ventricle (RV). On the other hand, the ventricular septum (VS) is visualized far better than the RV free wall on echocardiography. Furthermore, it has been shown that the VS is a morphologically and functionally bilayered structure divided by a bright line [5-7], and the right and left sides of the VS respond differently to ventricular overload [6].

Until recently, tissue Doppler imaging has been used for noninvasive assessment of myocardial performance, but tissue Doppler measurement is angle-dependent [3, 4]. A novel two-dimensional (2D) speckle-tracking echocardiography, which analyzes grayscale speckle patterns from frame to frame based on a pattern matching algorithm and is angle-independent, permits assessment of regional and global myocardial function in the fetus and newborn [8-11]. The accuracy and reproducibility of 2D speckle-tracking have been validated in normal pediatric subjects and patients with congenital heart disease [12].

It has been shown that gestational age, postnatal age and ventricular dimensions all influence myocardial properties measured by tissue Doppler and 2D speckle-tracking echocardiography [3, 4, 8-11]. These findings might reflect developmental characteristics in which the immature myocardium generates less active tension than the mature myocardium at similar muscle lengths [13, 14]. The use of 2D speckle-tracking echocardiography in preterm infants who are ill requires knowledge of the reference values specific to these patient population as well as the variations during the vulnerable transitional period soon after birth. The purpose of the present study was to serially assess myocardial performance of both sides of the VS, RV, and left ventricle (LV) during the transitional period in healthy preterm infants using 2D speckle-tracking echocardiography.

Methods

Study population

Infants weighing 750–2499 g born in our hospital and admitted to the neonatal intensive care unit from July 1, 2013 to August 31, 2014 were enrolled. Infants meeting the following criteria were excluded: 1) presence of chromosomal abnormality; 2) presence of congenital malformation (brain, heart, digestive tract); 3) small for gestational age; 4) resuscitation by bag and mask or intubation at birth; 5) oxygen administration of $FIO_2 > 0.3$; 6) symptomatic PDA; 7) use of inotropic agents; 8) plethora (hematocrit ≥ 65%); severe anemia (hematocrit < 35%); or 9) sepsis (at least one of positive blood culture, immunoglobulin M ≥ 20 mg/dL at birth, or use of immunoglobulin). This study was approved by the institutional review board of Iwate Medical University, after which written consent was obtained from the parents of all subjects prior to enrolment. The subject infants were managed according to standard practices.

Measurement of heart rate, mean blood pressure, respiratory rate, and SpO_2

Heart rate was measured using a heart rate monitor (IntelliVue MP70 Neonatal; Phillips Healthcare, Tokyo, Japan), and mean blood pressure was measured with an indirect oscillometric method (BX-10; Colin, Tokyo, Japan). The respiratory rate was counted visually. SpO_2 was measured with a pulse oximeter (Radical; Masimo, Irvine, CA, USA) attached to the right arm. These recordings were made in combination with echocardiography as described below and stored in a personal computer.

Echocardiographic measurements

Echocardiography was performed in the resting state without sedation by a single experienced investigator (YN) at 1, 3, 6, 9, 12, 24, 48, and 72 h after birth using an ultrasound system (iE33; Phillips Healthcare, Tokyo, Japan) and 7 and 12-MHz sector transducers.

Conventional echocardiographic measurement

According to the American Society of Echocardiography guidelines [15, 16], the following echocardiographic measurements were obtained using M-mode: LV end-diastolic (LVDd) and end-systolic diameters from the parasternal short axis view, and left atrial and aortic root diameters from the parasternal long axis view. LV shortening fraction (LVSF) and left atrial to aortic root (LA/Ao) ratio were obtained. Tricuspid annular plane systolic excursion (TAPSE) was measured from

the apical four-chamber view [17]. Right ventricular fractional area change (RVFAC) was obtained using 2D echocardiography from the apical four-chamber view. The time to peak flow (acceleration time, AcT) and right ventricular ejection time (RVET) were measured in the right ventricular outflow tract just below the pulmonary cusp by pulsed Doppler echocardiography in the parasternal short axis view, and AcT/RVET ratio was calculated [18]. Pulsed tissue Doppler imaging for the myocardial performance index (MPI) was obtained at the lateral tricuspid annulus and septal and lateral mitral annuli in the apical four-chamber view [15, 19]. All variables were measured for 3-5 heart beats at each study time, and the mean values were used in the analyses.

2D speckle-tracking echocardiography

The apical four-chamber view was used for measurements of 2D speckle-tracked peak systolic longitudinal strain (LS) of the VS, RV free wall, and LV at frame rates ranging from 101 to 192 frames/sec, 74 to 165 frames/sec, and 64 to 149 frames/sec, respectively. All images were recorded after optimizing scan width, gain, and dynamic range to maximize the image quality, and data for one cardiac cycle were stored in an archiving system (QLAB 9.1 software; Philips Healthcare, Tokyo, Japan) for later offline analysis. Care was taken to keep the ultrasound beam aligned parallel to the VS and RV free wall. Images were graded according to the scoring system [20], and only images graded as excellent or good were included in the following analysis. Regions of interest were manually positioned on the right and left sides of the VS separated by a bright line and the RV free wall, both at the middle part of the wall (Figure 1 and Figure 2a, b). The size of the sampling volume was 7.3 ± 2.0 (mean ± SD) mm for the right side of the VS, 7.3 ± 2.0 mm for the left side of the VS, and 10.9 [10.0-12.4] (median [inter-quartile range]) mm for the RV free wall. For measurement of global LV peak LS, a semi-automatic system traced the endocardial and myocardial borders. Segmental strain is represented by six different color-coded curves, and global LS is represented by the dotted white curve (Figure 2c). The semi-automatic tracking was visually inspected before accepting the results, and the tracing points were manually repositioned in most cases. Since systolic LS is defined as the percent shortening of the myocardium during systole, more negative LS values indicate more shortening/contraction of the tissue. In this article, “LS is larger” when LS values are more negative in intergroup comparisons.

Evaluation of ductus arteriosus and foramen ovale

The ductus arteriosus was observed using color Doppler echocardiography at each time point of the study, and cases were judged patent when continuous ductal shunt flow was seen from the aorta to the main pulmonary artery. The foramen ovale was judged patent when left to right atrial shunt flow was observed.

Statistical analysis

All data are expressed as means ± standard deviation (SD) or median [inter-quartile range] according to the data distribution unless otherwise indicated. Analysis of variance with the Tukey correction or Friedman test was done for intragroup comparisons by time after birth of each type of data as appropriate. The *t*-test was used for intergroup comparisons by site and for comparisons between study patients and the patients in whom measurements could not be made. To analyze factors associated with echocardiographic measurements, multiple regression analysis was done with echocardiographic indices at each time after birth as the dependent variable, and sex, gestational age, birth weight, mode of delivery, oxygen administration, use of nasal directional positive airway pressure (n-DPAP), and PDA at each time after birth as independent variables. Conventional echocardiographic measurements affecting LS were analyzed at each time point of the study. Person's correlation coefficient was obtained for regional LS values.

The reproducibility of strain measurement was assessed in 10 randomly selected subjects using Bland-Altman plot analysis [bias and 95% limits of agreement and intraclass correlation coefficient (ICC)]. For intra-observer variability, data were analyzed twice, 8 weeks apart. Interobserver variability was assessed by analyzing data from two separate observers blinded to each other's results. Statistical analysis was done using SPSS Ver. 20 for Windows (SPSS, Tokyo, Japan) with a significance level of $p<0.05$ (two-sided).

Results

Characteristics of the patients (Table 1)

Eighty-four preterm, low birth weight infants weighing 750–2499 g were admitted to our hospital during the study period, and exclusion criteria applied to 49 of them. Of the remaining 35, measurements could not be made for 14 infants because no examiner was present. As a result, the subjects were 21 infants (12 boys, 9 girls), including two sets each of twins and triplets. The gestational

age of the subjects was 33 ± 2 weeks (range, 28–36 weeks), and birth weight was 1913 ± 213 g (range, 899–2490 g). Eleven of the 21 subjects were diagnosed with transient tachypnea of the newborn or apnea of prematurity, and oxygen was administered ($FIO_2 \leq 0.3$) within the incubator or an oxygen hood, and nine subjects received n-DPAP within 72 h after birth. No apnea attacks occurred during measurements. There were no differences in clinical characteristics between study patients and the patients in whom measurements could not be made (n=14).

Changes in heart rate, mean blood pressure, respiratory rate, and SpO_2 over time (Figure 3)

Heart rate decreased significantly from 163 [154-182] bpm at 1 h to 137 [130-148] bpm at 72 h of age ($p<0.001$). Mean blood pressure increased significantly from 39 [35-45] mmHg at 1 h to 45[41-51] mmHg at 72 h of age ($p<0.01$). Respiratory rate and SpO_2 did not change significantly during the first 72 h of life.

Changes in standard echocardiographic measurements (Table 2)

Echocardiography was performed at 1.0 [0.9-1.2] h, 3.0 [3.0-3.2] h, 6.0 [6.0-6.1] h, 9.0 [9.0-9.5] h, 12.0 [11.9-12.3] h, 24.3 [24.0-25.8] h, 48.4 [47.6-49.7] h, and 72.0 [71.5-78.0] h after birth. The LA/Ao ratio decreased significantly from 1.5 ± 0.3 at 1 h to 1.2 ± 0.2 at 9 h ($p=0.028$), 1.3 ± 0.2 at 24 h ($p=0.049$), and 1.1 ± 0.2 at 48 h ($p=0.001$). RVFAC increased from 38.5 ± 9.8 at 1 h to 42.1 ± 8.9 at 48 h ($p=0.017$), and 47.7 ± 3.6 at 72 h ($p=0.002$). The AcT/RVET ratio increased significantly from 0.21 ± 0.05 at 1 h to 0.33 ± 0.09 at 24 h ($p=0.005$), 0.35 ± 0.10 at 48 h ($p<0.001$), and 0.31 ± 0.10 at 72 h ($p=0.002$). The LVDd, LVSF and TAPSE did not change during the 72 h after birth. Tissue Doppler-derived MPI at the three measurement points did not change during the study period.

Changes in 2D speckle-tracking strain measurements (Table 2 and Figure 4)

The bright line was visible in the middle of the VS in the four-chamber view in all subjects. The peak LS on the right side and the left side of the VS and RV free wall did not change during the 72 h after birth. The peak LS was significantly larger on the left side of the VS than on the right side of the VS at 1 h (-22.7 ± 5.7% vs. -17.9 ± 4.5%, $p=0.047$), 48 h (-19.8 ± 3.1% vs. -17.3 ± 4.5%, $p=0.048$), and 72 h (-20.9 ± 3.0% vs. -14.7 ± 4.6%, $p=0.002$). The peak LS remained significantly larger on the RV free wall than on the right side of the VS throughout the study period ($p<0.01$). The global LV peak

LS did not change during the first 72 h of life.

Feasibility and reproducibility of 2D speckle-tracking strain measurements (Table 3)

Strain measurement was feasible in the majority of acquired images: 141/150 images (94%) of the VS, 118/137 images (86%) of the RV free wall, and 132/144 images (92%) of the LV. The feasibility of images of the VS was significantly higher compared to that of the RV free wall (p=0.01). For intra-observer reproducibility, Bland-Altman analysis showed minimal bias (<10%), and the ICC showed moderate to substantial agreement in four strain measurement sites (0.560-0.744). For inter-observer reproducibility, Bland-Altman analysis showed minimal bias (<10%), and the ICC showed substantial agreement in three speckle-tracking strain measurement sites (0.717-0.758), except the RV free wall, in which the ICC showed modest agreement of 0.455.

Changes in the ductus arteriosus and foramen ovale over time

PDA was seen in 21 infants at 1 h, 18 infants at 3 h, 17 infants at 6 h, 14 infants at 9 h, 13 infants at 12 h, 7 infants at 24 h, 3 infants at 48 h, and 1 infant at 72 h. Compared with 1 h, cases of patency were significantly decreased at 12 h (p=0.033), 24 h (p<0.001), 48 h (p<0.001), and 72 h (p<0.001). Symptomatic PDA was not seen in any case. The left to right shunt through the foramen ovale was observed constantly in all infants during the study period.

Analysis of factors affecting echocardiographic measurements and correlations of regional strain values (Table 4, 5)

On multiple regression analysis, LVDd and TAPSE appeared significantly associated with birth weight. LVDd was associated with PDA at 12 h and use of n-DPAP at 48 h. Peak LS on the right and left sides of the VS was significantly associated with use of n-DPAP in an opposite direction. The associations between peak LS and oxygen administration were inconsistent between the right side of the VS and the RV free wall. The RV free wall peak LS and the global LV peak LS were significantly associated with MPI lateral tricuspid and MPI septal mitral, respectively. The peak LS on the right side of the VS was associated with TAPSE, and the RV free wall peak LS was associated with AcT/RVET. Correlation analysis showed a significant correlation between peak LS on the right side VS and on the RV free wall at 72 h (r= 0.593, p<0.001), and peak LS on the left side of the VS and on the global LV at

72 h (r= 0.55, p=0.007).

Discussion

In the present study, peak LS was maintained at the four analyzed regions during the first 72 h of life despite significant hemodynamic changes, including decreased heart rate and increased mean blood pressure, and decreased pulmonary artery pressure and PDA closure as assessed by conventional echocardiography. The peak LS was significantly larger on the left side of the VS than on the right side of the VS at 1 h, 48 h, and 72 h after birth. To the best of our knowledge, this is the first report of serial measurement of systolic LS on both sides of the VS, RV, and LV in preterm infants using 2D speckle-tracking echocardiography.

There are few studies of 2D speckle-tracking echocardiography examining fetal or neonatal myocardial performance. In normal fetuses, Di Salvo et al. [8] studied LS in RV, VS and LV during 20-32 weeks of gestation and found significant correlations between gestational age and LS (n=100). In healthy term infants, Schubert et al. [9] found that LS values at a mean 170 (range 135-207) h after birth were significantly larger in the RV than in the LV and VS (n=30). These values were significantly decreased compared to fetal values of the same infants at 28 weeks of gestation. Jain et al. [10] reported that RV free wall LS was maintained between 15 ± 2 h and 35 ± 2 h of age in healthy term newborns (n=50). In preterm infants, Levy et al. [11] reported high feasibility and reproducibility of RV LS measurement in 50 infants with 27 ± 1 gestational weeks and 0.96 ± 0.2 kg birth weight at 32 weeks (1.42 ± 0.3 kg body weight) and at 36 weeks postmenstrual age (2.21 ± 0.3 kg body weight), but exact values and comparisons between LS measurements at two time points were not included. Using tissue Doppler imaging, it has been found that LS of the VS, RV, and LV did not change between 10 h and 45 h post-delivery in 54 preterm infants with a median gestation and birth weight of 26.5 weeks and 915 g, respectively. All infants in this study received early surfactant prior to the first echocardiography, 61% received mechanical ventilation, and all infants had large unconstricted PDA at 10 h of age [4]. The results of the present study and those of previous studies [4, 9, 10] might indicate that abrupt changes in LS occur at the time of cord clumping and removal of the placenta and that LS is maintained at the VS, RV, and LV to some extent despite significant hemodynamic changes during the transition period in preterm infants. This study reveals that the peak LS of the VS, RV, and LV is relatively independent

of hemodynamic changes and can therefore serve as an index for myocardial evaluation during the transition in preterm infants.

Longitudinal deformation was significantly larger on the left side of the VS than on the right side of the VS at 1 h, 48 h, and 72 h after birth. This is contrary to previous findings from normal subjects [5, 7]. Boettler et al. [5] found similar LS on the right and on the left VS in healthy adults (n=30, ages ranged 18-53 years) using Doppler myocardial imaging. Hayabuchi et al. [7] reported similar findings in normal children (n=132, age 1.0-10.0 years) using 2D speckle-tracking echocardiography. They speculated that the close connection of both sides of the VS prevented independent longitudinal movement, and each side affected the other. Interestingly, however, Hayabuchi et al. [6] documented in another report that in patients (n=22, age 9.0 ± 4.2 years) with a hemodynamically significant atrial septal defect, LS on both sides of the VS was significantly larger than in controls. Furthermore, LS on the left side of the VS was significantly larger than on the right side of the VS.

A geometric model showed that the right and left sides of the VS respond differently to various conditions [21]. At birth, the systemic vascular resistance abruptly increases with discontinuation of the low resistance placental circulation. Data for right ventricular preload are less conclusive, but it seems that preload drops with clamping of the umbilical cord and rises within hours to supra-fetal levels [9]. The rapid decrease in pulmonary vascular resistance and the increase in pulmonary blood flow augments preload to the left side of the heart. The increased ductal left-to-right shunt also enhances venous return to the left atrium, which will raise left atrial pressure. If the foramen ovale is patent, an atrial left-to-right shunt may raise right ventricular output to levels above those of systemic venous return [14, 22]. All subjects in the present study had a patent foramen ovale until 72 h of age. Although the magnitude of the shunt was not quantified, both ductal and atrial shunts might have caused a significant right ventricular volume overload and affected LS of the VS along with left ventricular pressure and volume overload. It is also plausible that inotropic stimulation with the catecholamine surge induced by delivery affects strain measurements immediately after birth. During the following days, the loading conditions of the right and left ventricles further change along with the further decrease in pulmonary vascular resistance and closure of the ductal shunt. All these responses might have altered the myocardial performance of the RV and LV and affected the longitudinal deformation of the VS. The different deformation between the bilayered VS might indicate the presence of the

delicate pressure and volume adaptation, which is not shown on the RV free wall and global LV deformation.

The peak LS on the right and left sides of the VS was significantly associated with use of n-DPAP at 48 h and 72 h, respectively, in an opposite direction. The global LV peak LS and LVDd were also significantly associated with use of n-DPAP at 6 h and 48 h, respectively. To our knowledge, the impact of n-DPAP on myocardial deformation in preterm infants was not addressed previously. In adult patients with obstructive sleep apnea, a few studies demonstrated that chronic therapy using n-DPAP improved both right and left ventricular LS [23, 24]. However, the mechanisms by which n-DPAP alter the hemodynamic status of patients are complex. It has been shown that incremental positive end-expiratory pressure affects the right and left ventricular LS differently and result in a change in right and left ventricular dimensions inversely in adult patients [25]. Since there were significant correlations between LS on the right side of the VS and the RV free wall and between LS on the left side of the VS and global LV at 72 h after birth, the present results suggest that the right and left sides of the VS respond differently to the multiple and complex cardiopulmonary transitions from fetal to neonatal life in preterm infants and that peak LS on the right and left sides of VS might be a sensitive parameter to detect subtle changes in regional myocardial performance in patients with n-DPAP.

The feasibility and reproducibility of 2D strain measurement in the present study were in agreement with previous studies [6-11, 26], but feasibility was lower for the RV free wall than for the VS. For inter-observer reproducibility, the ICC showed substantial agreement on both sides of the VS and the LV, whereas the ICC for the RV free wall was modest. These results might be related to the method of image acquisition of the RV; a standard apical four-chamber view was used in order to avoid interfering with respiration of small infants. The RV myofiber architecture is characterized by dominant longitudinal layers aligned from the base to apex, which allow greater longitudinal than radial shortening and twisting and rotational movements [10]. It is important to define the full extent of the RV free wall to avoid the loss of the optimum number of RV segments through the cardiac cycle for tracking the longitudinal movement [10, 27]. The standard apical four-chamber view might have failed to include the entire RV free wall in its imaging plane and led to poor speckle-tracking. Recently, an RV-focused view has been advocated for high clinical feasibility and reproducibility [10, 15].

Study limitations

Several study limitations should be addressed. First, this study included a small number of infants in a single center, and a larger study is needed to determine the myocardial response during the transitional period in preterm infants. Second, a standard apical four-chamber view was used and not an RV-focused view or other view, which might have affected LS measurements of the RV free wall. Third, the focus was on mid-ventricular regions of the VS and RV free wall. The myofibers in the base and mid regions of the VS have longitudinal orientation, and the fibers of its apex have circumferential orientation, according to Torrent-Guasp et al. [28]. A recent meta-analysis showed a significant base to apex segmental strain gradient in the RV free wall in normal children [29]. Comparisons with strain values from different regions are necessary to determine the global myocardial performance in preterm infants. Fourth, in this study, we measured the LS and analyzed its correlation with clinical and conventional echocardiographic characteristics. However, the circumferential strain of both sides of VS might have the different pattern in this period. Hayabuchi et al. [6] reported that the longitudinal deformation of both sides of VS was similar in normal children, whereas circumferential strain was significantly different. Finally, a commercially available ultrasound system and vendor-customized software, which are different from those used in most previous pediatric studies, were used [8-10]. Since strain measurements are reported to be significantly different for each of the vendors [30], care should be taken when comparing results between studies.

Conclusion

Preterm infants without mechanical ventilation, inotropic agents, or symptomatic PDA showed stable LS on both sides of the VS, RV free wall, and LV despite hemodynamically significant changes during the first 72 h of life. LS was significantly larger on the left side of the VS than on the right side of the VS at 1 h, 48 h, and 72 h after birth, and the responsible mechanisms and clinical implications should be elucidated in further studies.

Acknowledgment

This study was approved by the institutional review board of Iwate Medical University (H25-63).

Conflict of interest

Yurie Nasu, Kotaro Oyama, Satoshi Nakano, Atsushi Matsumoto, Wataru Soda, Shin Takahashi,

and Shoichi Chida declare that they have no conflict of interest.

Human rights statement and informed consent

All procedures followed were in accordance with the ethical standards of the institutional review board of Iwate Medical University and with the Helsinki Declaration of 1975, as revised in 2000. Informed consent was obtained from the parents of all subjects prior to enrolment.

References

1. Kluckow M, Seri I. Clinical presentations of neonatal shock: the very low birth weight neonate during the first postnatal day. In: Kleinman CS, Seri I, Polin RA, editors. Hemodynamics and Cardiology. Neonatology Questions and Controversies. 2nd ed. Philadelphia, Elsevier Saunders; 2012. p. 237-67.
2. El-Khuffash AF, Jain A, Dragulescu A, et al. Acute changes in myocardial systolic function in preterm infants undergoing patent ductus arteriosus ligation: a tissue Doppler and myocardial deformation study. J Am Soc Echocardiogr. 2012;25:1058-67.
3. Lee A, Nestaas E, Liestol K, et al. Tissue Doppler imaging in very preterm infants during the first 24 h of life: an observational study. Arch Dis Child Fetal Neonatal Ed. 2014;99:F64-9.
4. James AT, Corcoran JD, Jain A, et al. Assessment of myocardial performance in preterm infants less than 29 weeks gestation during the transitional period. Early Hum Dev. 2014;90:829-35.
5. Boettler P, Claus P, Herbots L, et al. New aspects of the ventricular septum and its function: an echocardiographic study. Heart. 2005;91:1343-48.
6. Hayabuchi Y, Sakata M, Ohnishi T, et al. A novel bilayer approach to ventricular septal deformation analysis by speckle tracking imaging in children with right ventricular overload. J Am Soc Echocardiogr. 2011;24:1205-12.
7. Hayabuchi Y, Sakata M, Kagami S. Assessment of the helical ventricular myocardial band using standard echocardiography. Echocardiography. 2014. doi:10.1111/echo.12624.
8. Di Salvo G, Russo MG, Paladini D, et al. Two-dimensional strain to assess regional left and right ventricular longitudinal function in 100 normal fetuses. Eur J Echocardiogr. 2008;9:754-6.
9. Schubert U, Müller M, Norman M, et al. Transition from fetal to neonatal life: changes in cardiac function assessed by speckle-tracking echocardiography. Early Hum Dev. 2013;89:803-8.
10. Jain A, Mohamed A, El-Khuffash A, et al. A comprehensive echocardiographic protocol for assessing neonatal right ventricular dimensions and function in the transitional period: normative data and Z scores. J Am Soc Echocardiogr. 2014;27:1293-304.
11. Levy PT, Holland MR, Sekarski TJ, et al. Feasibility and reproducibility of systolic right ventricular strain measurement by speckle-tracking echocardiography in premature infants. J Am Soc Echocardiogr. 2013;26:1201-13.
12. Singh GK, Cupps B, Pasque M, et al. Accuracy and reproducibility of strain by speckle tracking in

pediatric subjects with normal heart and single ventricular physiology: a two-dimensional speckle-tracking echocardiography and magnetic resonance imaging correlative study. J Am Soc Echocardiogr. 2010;23:1143-52.

13. Friedman WF. The intrinsic physiologic properties of the developing heart. Prog Cardiovasc Dis 1972;15:87-111.
14. Rudolph AM. Congenital Diseases of the Heart. Clinical-physiological considerations. 3rd ed. West Sussex: Wiley-Blackwell: 2009.
15. Rudski LG, Lai WW, Afilalo J, et al. Guidelines for the echocardiographic assessment of the right heart in adults: a report from the American Society of Echocardiography. Endorsed by the European Association of Echocardiography, a registered branch of the European Society of Cardiology, and the Canadian Society of Echocardiography. J Am Soc Echocardiogr. 2010;23:685-713.
16. Mertens L, Seri I, Marek J, et al. Targeted neonatal echocardiography in the neonatal intensive care unit: practice guidelines and recommendations for training. Writing group of the American Society of Echocardiography (ASE) in collaboration with the European Association of Echocardiography (EAE) and the Association for European Pediatric Cardiologists (AEPC). J Am Soc Echocardiogr. 2011;24:1057-78.
17. Koestenberger M, Ravekes W, Everett AD, et al. Right ventricular function in infants, children and adolescents: reference value of the tricuspid annular plane systolic excursion (TAPSE) in 640 healthy patients and calculation of z score values. J Am Soc Echocardiogr. 2009;22:715-9.
18. Kitabatake A, Inoue M, Asao M, et al. Noninvasive evaluation of pulmonary hypertension by a pulsed doppler technique. Circulation. 1983;68:302-9.
19. Mejia AAS, Simpson KE, Hildebolt CF, et al. Tissue Doppler septal Tei index indicates severity of illness in pediatric patients with congestive heart failure. Pediatr Cardiol. 2014;35:411-8.
20. Colan SD, Shirali G, Margossian R, et al. The ventricular volume variability study of the pediatric heart network: study design and impact of beat averaging and variable type on the reproducibility of echocardiographic measurements in children with chronic dilated cardiomyopathy. J Am Soc Echocardiogr. 2012;25:842-54.
21. Beyar R, Dong SJ, Smith ER, at al. Ventricular interaction and septal deformation: a model compared with experimental data. Am J Physiol. 1993;265:H2044-56.

22. Evans N, Iyer P. Assessment of ductus arteriosus shunt in preterm infants supported by mechanical ventilation: effect of interatrial shunting. J Pediatr, 1994;125:778-85.
23. Haruki N, Takeuchi M, Kanazawa Y, et al. Continuous positive airway pressure ameliorates sleep-induced subclinical left ventricular systolic dysfunction: demonstration by two-dimensional speckle-tracking echocardiography. Eur J Echocardiogr. 2010;11:352-8.
24. Hammerstingl C, Schueler R, Wiesen M, et al. Impact of untreated obstructive sleep apnea on left and right ventricular myocardial function and effects of CPAP therapy. PLOS ONE. 2013.doi:10.1371/journal.pone.0076352
25. Franchi F, Faltoni A, Cameli M, et al. Influence of positive end-expiratory pressure on myocardial strain assessed by speckle tracking echocardiography in mechanically ventilated patients. BioMed Res Int. 2013. Doi:10.1155/2013/918548.
26. Fukuda Y, Tanaka H, Sugiyama D, et al. Utility of right ventricular free wall speckle-tracking strain for evaluation of right ventricular performance in patients with pulmonary hypertension. J Am Soc Echocardiogr. 2011;24:1101-8.
27. Giusca S, Dambrauskaite V, Scheurwegs C, et al. Deformation imaging describes right ventricular function better than longitudinal displacement of the tricuspid ring. Heart. 2010;96:281-88.
28. Torrent-Guasp F, Ballester M, Buckberg GD, et al. Spatial orientation of the ventricular muscle band: physiologic contribution and surgical implication. J Thorac Cardiovasc Surg. 2001;122:389-92.
29. Levy PT, Mejia AAS, Machefsky A, et al. Normal ranges of right ventricular systolic and diastolic strain measures in children: a systematic review and meta-analysis. J Am Soc Echocardiogr. 2014;27:549-60.
30. Takigiku K, Takeuchi M, Izumi C, et al. Normal range of left ventricular 2-dimensional strain –Japanese ultrasound speckle tracking of the left ventricle (JUSTICE) study- Circ J. 2012;76:2623-32.

Figure Legends

Figure 1. Apical four-chamber view of the ventricular septum

This four-chamber view shows the right side (*yellow*) and the left side (*green*) of the ventricular septum separated by the bright line (arrow). *RV* right ventricle, *LV* left ventricle, *LA* left atrium.

Figure 2. Apical four-chamber view of the ventricular septum, right ventricular free wall, and global left ventricle

(a) Longitudinal speckle-tracking strain imaging of the right side (*yellow*) and left side (*green*) of the ventricular septum. (b) Right ventricular free wall longitudinal speckle-tracking strain curve. (c) Left ventricular longitudinal speckle-tracking strain curve. Segmental longitudinal strain is graphically represented by six different color-coded curves, and global longitudinal strain is graphically represented by the white dotted curve.

Figure 3. Changes in heart rate, mean blood pressure, respiratory rate, and SpO_2

The box shows the median (central line) with interquartile range (25–75th percentile) and the whisker represents the 5–95th percentile.

▥ , heart rate; ▨ , mean blood pressure; ■ , respiratory rate; □ , SpO_2.

**p < 0.01, ***p<0.001.

Figure 4. Changes in 2D speckle-tracking strain measurements on the right side and the left side of the ventricular septum

The peak longitudinal strain is significantly larger on the left side than on the right side of the ventricular septum at 1, 48, and 72 h after birth. The bar shows the mean ± standard deviation.

● , right side of the ventricular septum; ○ , left side of the ventricular septum.

*p < 0.05, **p < 0.01.

Table 1. Subjects' characteristics

Variable	Value
Number	21
Gestational week	33 ± 2
Birth weight (g)	1913 ± 213
Male	12 (57)
Reason of delivery	
PROM	4 (20)
Premature delivery	7 (33)
Premature separation	1 (5)
PIH	2 (9)
Fetal distress	3 (15)
TTTS	2 (9)
triplet	2 (9)
Mode of delivery	
Vaginal delivery	4 (20)
Caesarean section	17 (80)
Apgar score	
≤ 7 (1 min)	7 (33)
≤ 7 (5 min)	2 (9)
O_2 administration (FiO2 ≤ 0.3)	11 (52)
n-DPAP	9 (43)

Values indicate mean ± standard deviation or number (%)
PROM premature rupture of the membranes, *PIH* pregnancy-induced hypertension, *TTTS* twin-to-twin transfusion, *n-DPAP* nasal directional positive airway pressure.

Table 2. Echocardiographic data during the first 72 h of life

Postnatal age (h)	1	3	6	9
LVDd (cm)	1.6 ± 0.2	1.6 ± 0.2	1.6 ± 0.3	1.5 ± 0.2
LVSF (%)	32.0 [25.3-38.0]	28.0 [26.4-38.8]	28.5 [22.3-36.7]	28.7 [24.0-32.8]
LA/Ao	1.5 ± 0.3	1.3 ± 0.2	1.2 ± 0.3	1.2 ± 0.2 *
TAPSE (cm)	0.73 ± 0.10	0.69 ± 0.10	0.71 ± 0.07	0.66 ± 0.07
RVFAC (%)	38.5 ± 9.8	41.4 ± 6.3	31.9 ± 6.9	38.4 ± 8.5
AcT/RVET	0.21 ± 0.05	0.22 ± 0.04	0.27 ± 0.06	0.27 ± 0.09
MPI lateral tricuspid	0.47 ± 0.10	0.44 ± 0.10	0.47 ± 0.06	0.49 ± 0.08
MPI septal mitral	0.54 [0.45-0.70]	0.48 [0.39-0.56]	0.62 [0.57-0.67]	0.54 [0.50-0.58]
MPI lateral mitral	0.46 [0.42-0.54]	0.51 [0.50-0.57]	0.51 [0.40-0.60]	0.51 [0.43-0.61]
VSR peak LS (%)	-17.9 ± 4.5 †	-16.2 ± 4.3	-14.6 ± 4.6	-16.3 ± 4.0
VSL peak LS (%)	-22.7 ± 5.7	-17.6 ± 3.4	-16.5 ± 3.9	-19.0 ± 6.9
RVFW peak LS (%)	-22.0 ± 4.7 ‡	-21.9 ± 5.8 ‡	-19.3 ± 3.6 ‡	-22.4 ± 3.0 ‡
GLV peak LS (%)	-23.8 ± 4.0	-24.2 ± 4.1	-20.4 ± 6.2	-23.0 ± 2.0

Postnatal age (h)	12	24	48	72
LVDd (cm)	1.6 ± 0.2	1.5 ± 0.2	1.5 ± 0.1	1.5 ± 0.3
LVSF (%)	26.9 [25.6-30.8]	31.5 [26.9-37.2]	25.7 [22.8-31.3]	30.0 [28.6-31.5]
LA/Ao	1.2 ± 0.2	1.3 ± 0.2 *	1.1 ± 0.2 **	1.2 ± 0.3
TAPSE (cm)	0.75 ± 0.09	0.76 ± 0.07	0.70 ± 0.06	0.74 ± 0.10
RVFAC (%)	43.4 ± 5.9	41.5 ± 9.3	42.1 ± 8.9 *	47.7 ± 3.6 **
AcT/RVET	0.27 ± 0.07	0.33 ± 0.09 **	0.35 ± 0.10 ***	0.31 ± 0.10 **
MPI lateral tricuspid	0.44 ± 0.06	0.40 ± 0.12	0.46 ± 0.13	0.41 ± 0.07
MPI septal mitral	0.50 [0.42-0.59]	0.46 [0.38-0.53]	0.43 [0.38-0.53]	0.49 [0.48-0.56]
MPI lateral mitral	0.45 [0.40-0.55]	0.47 [0.41-0.49]	0.54 [0.50-0.60]	0.47 [0.40-0.56]
VSR peak LS (%)	-18.8 ± 3.9	-17.7 ± 4.6	-17.3 ± 4.5 †	-14.7 ± 4.6 ††
VSL peak LS (%)	-22.5 ± 5.4	-21.0 ± 5.1	-19.8 ± 3.1	-20.9 ± 3.0
RVFW peak LS (%)	-21.7 ± 5.0 ‡	-24.7 ± 4.7 ‡	-20.8 ± 2.6 ‡	-22.9 ± 5.1 ‡
GLV peak LS (%)	-24.9 ± 3.1	-23.4 ± 3.2	-23.8 ± 5.1	-24.9 ± 3.2

Data are presented as means ± standard deviation or medians [inter-quartile range].
LVDd left ventricular end-diastolic dimension, *LVSF* left ventricular shortening fraction, *LA/Ao* left atrial / aortic root ratio, *TAPSE* tricuspid annular plane systolic excursion, *RVFAC* right ventricular fractional area change, *AcT/RVET* acceleration time / right ventricular ejection time ratio, *MPI* myocardial performance index, *VSR* right side of ventricular septum, *VSL* left side of ventricular septum, *RVFW* right ventricular free wall, *GLV* global left ventricle, *LS* longitudinal strain.
*p < 0.05, **p < 0.01, ***p < 0.001 compared with 1 h after birth.
† VSR peak LS compared with VSL peak LS, p < 0.05.
†† VSR peak LS compared with VSL peak LS, p < 0.01.
‡VSR peak LS compared with RVFW peak LS, p < 0.01.

Table 3. Intra-observer and inter-observer variabilities

Intra-observer variability					
	1st	2nd			
	mean ± SD	mean ± SD	p value	Bias (95% LOA)	ICC
VSR peak LS (%)	-18.5 ± 4.2	-18.3 ± 4.3	0.919	0.2 (-7.9 to 8.3)	0.560
VSL peak LS (%)	-20.9 ± 4.4	-20.0 ± 3.8	0.628	0.9 (-4.9 to 6.7)	0.744
RVFW peak LS (%)	-23.3 ± 3.6	-21.9 ± 3.6	0.389	1.4 (-4.3 to 7.1)	0.628
GLV peak LS (%)	-26.0 ± 2.2	-24.7 ± 2.8	0.263	1.3 (-1.5 to 4.0)	0.739

Inter-observer variability					
	Observer 1	Observer 2			
	mean ± SD	mean ± SD	p value	Bias (95% LOA)	ICC
VSR peak LS (%)	-18.3 ± 4.3	-17.4 ± 3.1	0.576	1.0 (-4.1 to 6.0)	0.758
VSL peak LS (%)	-20.0 ± 3.8	-20.4 ± 3.0	0.814	- 0.4 (-5.6 to 4.9)	0.717
RVFW peak LS (%)	-21.9 ± 3.6	-21.0 ± 4.5	0.604	1.0 (-7.5 to 9.4)	0.455
GLV peak LS (%)	-24.7 ± 2.8	-25.2 ± 3.7	0.736	- 0.5 (-4.9 to 4.0)	0.717

VSR right side of ventricular septum, *VSL* left side of ventricular septum, *RVFW* right ventricular free wall, *GLV* global left ventricle, *LS* longitudinal strain, *LOA* limits of agreement, *ICC* intraclass correlation coefficient.

Table 4. Clinical factors affecting echocardiographic measurements

Postnatal age (h)	Dependent variable	Independent variable	β	p	R^2
1	TAPSE	Birth weight	0.921	<0.001	0.734
6	GLV peak LS	Use of n-DPAP	0.59	0.002	0.630
	RVFW peak LS	O_2 administration	0.729	0.002	0.495
12	LVDd	Birth weight	0.636	0.001	0.534
		PDA	0.495	0.005	0.534
48	LVDd	Use of n-DPAP	- 0.525	0.004	0.536
	VSR peak LS	Use of n-DPAP	- 0.498	0.018	0.514
		O_2 administration	- 0.728	0.002	0.514
72	LVDd	Birth weight	0.769	<0.001	0.568
	VSL peak LS	Use of n-DPAP	0.616	0.014	0.325

β, standardized coefficient; R^2, coefficient of determination
TAPSE tricuspid annular plane systolic excursion, *RVFW* right ventricular free wall, *VSR* right side of ventricular septum, *VSL* left side of ventricular septum, *LVG* global left ventricle, *LS* longitudinal strain, *n-DPAP* nasal directional positive airway pressure, *PDA* patent ductus arteriosus.

Table 5. Conventional echocardiographic measurements affecting speckle-tracking echocardiographic measurements

Postnatal age (h)	Dependent variable	Independent variable	β	p	R^2
1	GLV peak LS	MPI septal mitral	1.017	<0.001	0.827
	VSR peak LS	TAPSE	- 0.749	0.002	0.525
	RVFW peak LS	MPI lateral tricuspid	0.583	0.029	0.285
6	GLV peak LS	MPI septal mitral	0.498	0.047	0.378
12	RVFW peak LS	AcT/RVET	0.534	0.033	0.235

β, standardized coefficient; R^2, coefficient of determination
GLV global left ventricle, *VSR* right side of ventricular septum, *RVFW* right ventricular free wall, *LS* longitudinal strain, *MPI* myocardial performance index, *TAPSE* tricuspid annular plane systolic excursion, *AcT/RVET* acceleration time / right ventricular ejection time ratio.

Figure 1.

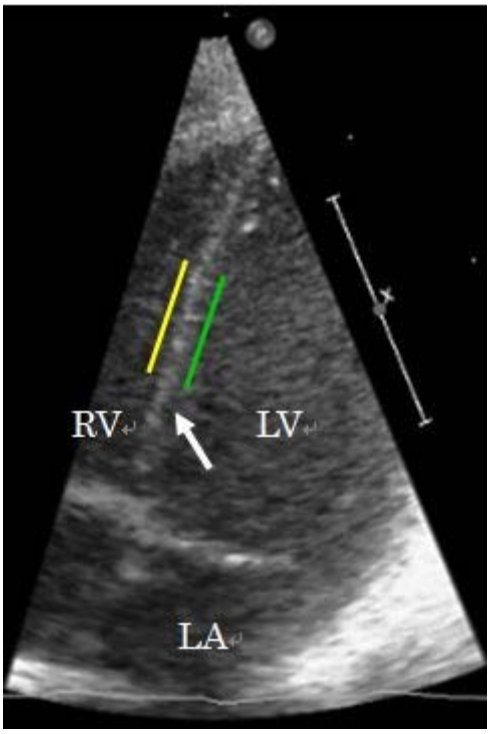

Figure 2.

(A)

1/1
13:07:58
HR = 157 bpm
5 mm
Strain (%)
-1
-4
-7
-10
-13
-16
-19
-22
-25
0.42
0.46
0.50
0.54
0.58
0.62
0.66
0.70
0.74
0.78
Time (sec)

Figure 2.

(B)

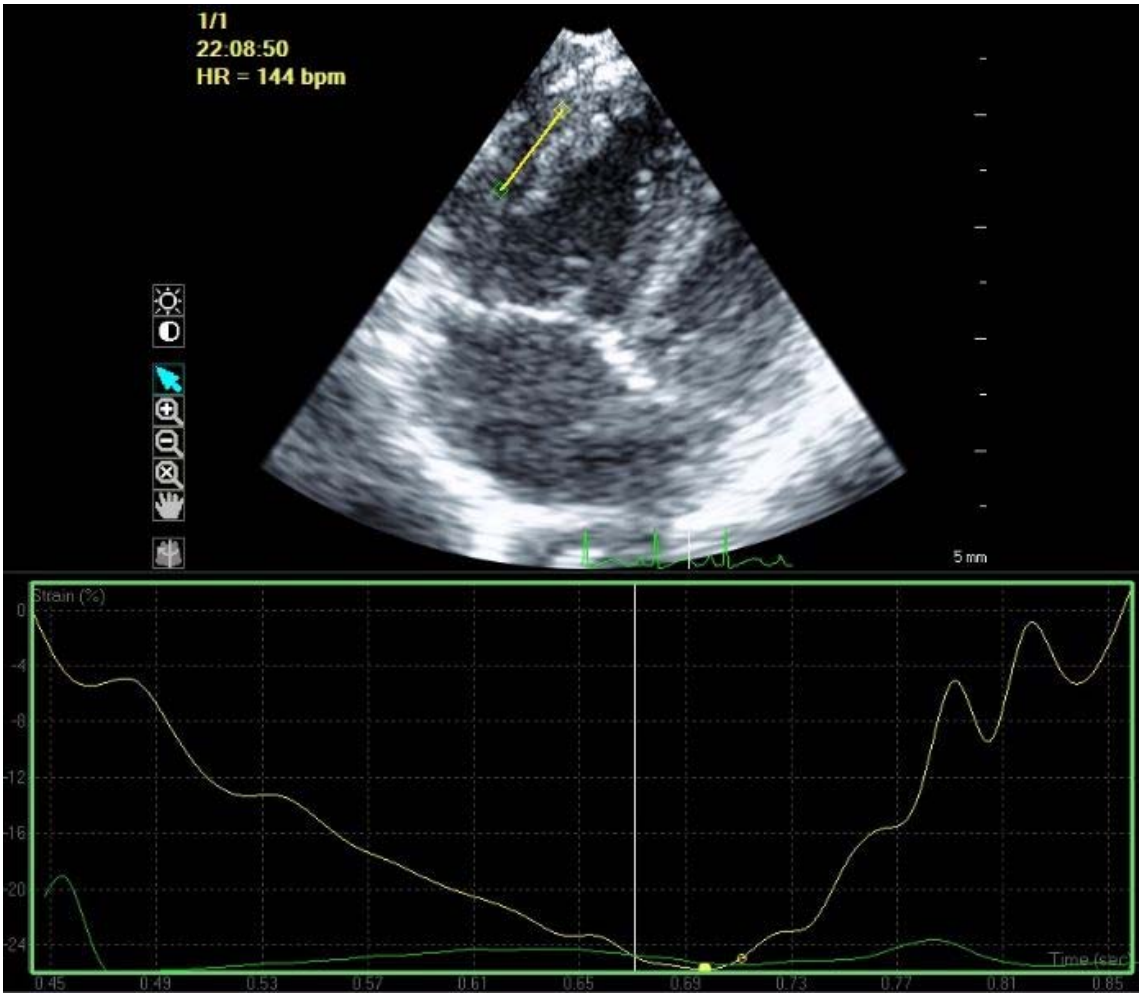
1/1
22:08:50
HR = 144 bpm
5 mm
Strain (%)
0
-4
-8
-12
-16
-20
-24
0.45
0.49
0.53
0.57
0.61
0.65
0.69
0.73
0.77
0.81
0.85
Time (sec)

Figure 2.

(C)

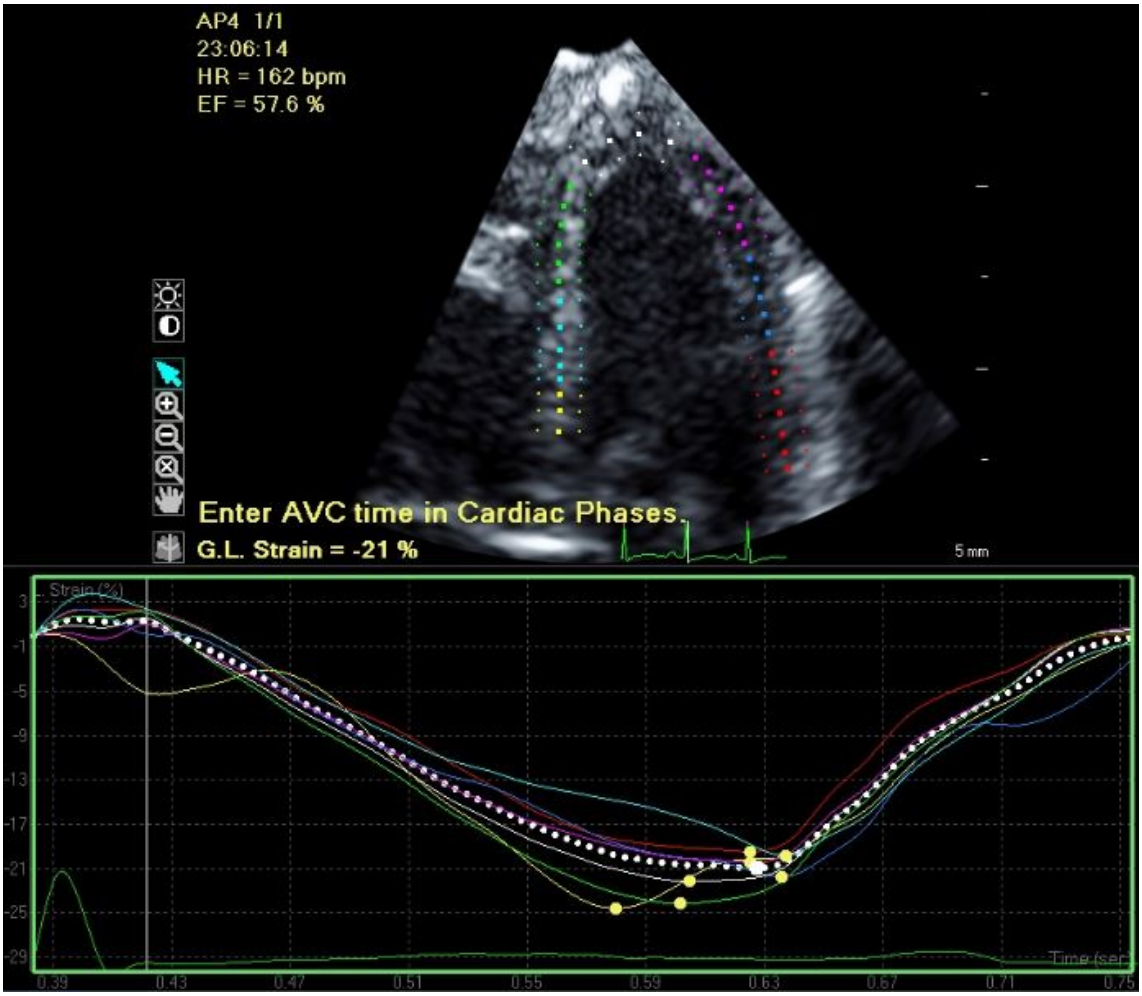
AP4 1/1
23:06:14
HR = 162 bpm
EF = 57.6 %
Enter AVC time in Cardiac Phases.
G.L. Strain = -21 %
5 mm
Strain (%)
3
-1
-5
-9
-13
-17
-21
-25
-29
0.39
0.43
0.47
0.51
0.55
0.59
0.63
0.67
0.71
0.75
Time (sec)

Figure 3.

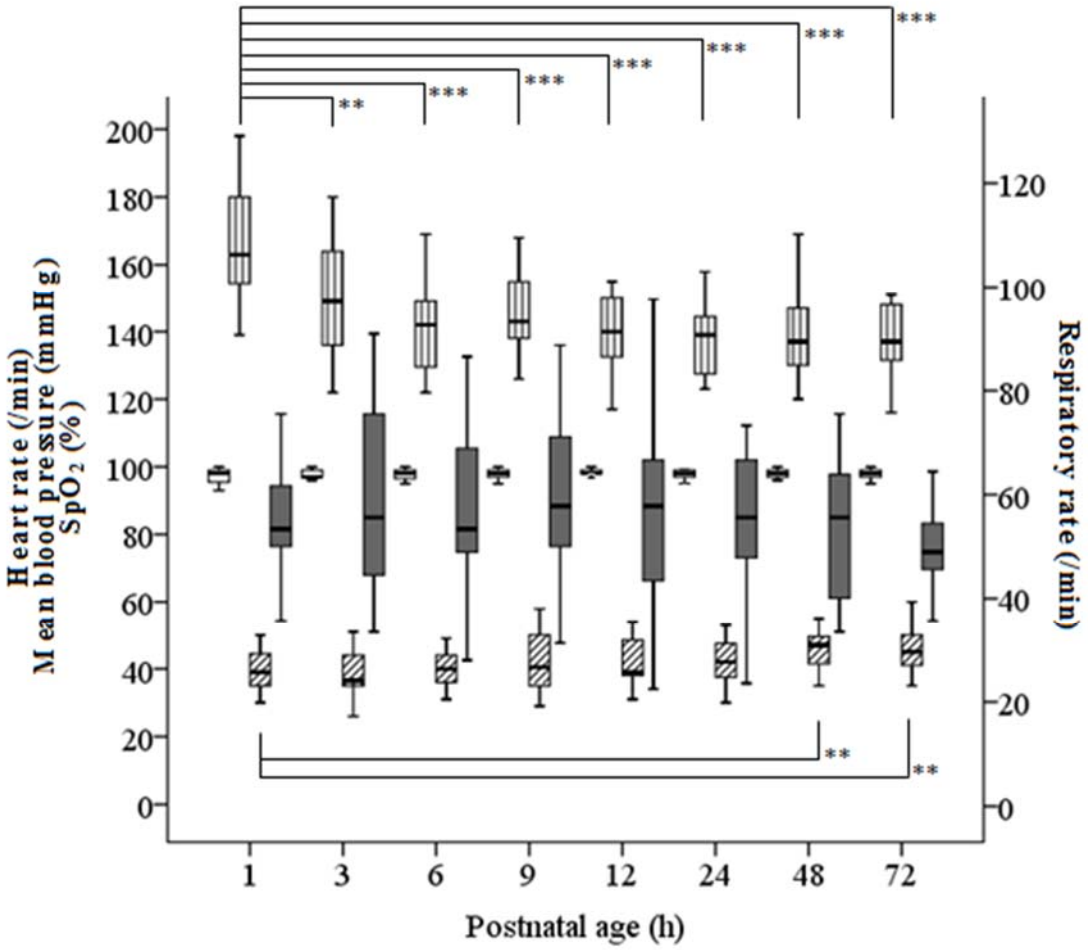
Heart rate (/min)
Mean blood pressure (mmHg)
SpO2 (%)
Respiratory rate (/min)
Postnatal age (h)
1
3
6
9
12
24
48
72
0
20
40
60
80
100
120
140
160
180
200
0
20
40
60
80
100
120
**
***
***
***
***
***
**
**

Figure 4.

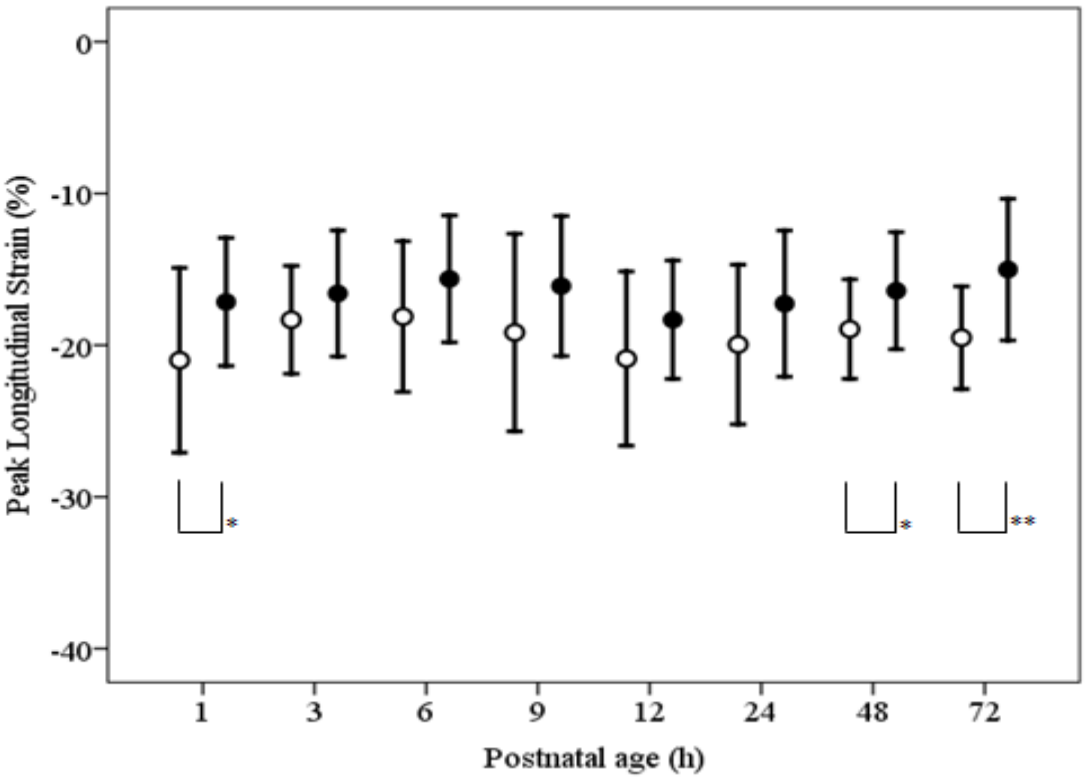
0
-10
-20
-30
-40
Peak Longitudinal Strain (%)
*
*
**
1
3
6
9
12
24
48
72
Postnatal age (h)